



Received on 09 March, 2013; received in revised form, 12 June, 2013; accepted, 21 July, 2013; published, 01 August, 2013

IDENTIFICATION OF POTENT VIRTUAL LEADS AS TOPOISOMERASE-II INHIBITORS USING PHARMACOPHORE MODELLING, MOLECULAR DOCKING AND ADME STUDIES

Sanal Dev¹ and Sunil R. Dhaneshwar*²

Department of Pharmaceutical Chemistry, B.V.D.U Poona College of Pharmacy, Pune, Maharashtra, India

Department of Pharmaceutical Chemistry, Ras Al Khaimah Medical and Health Sciences University, College of Pharmaceutical Sciences, Ras Al Khaimah- 11172, UAE

Keywords:

Pharmacophore, 3-D QSAR, Topoisomerase inhibitor, Pyridine, Docking

Correspondence to Author:

Warid Khayata

Faculty of pharmacy- university of Aleppo. Department of analytical and food chemistry, Syria

E-mail: sunil.dhaneshwar@gmail.com

ABSTRACT: Topoisomerase enzymes are highly expressed in cells which undergo rapid multiplication. Inhibition of this enzyme represents a potential therapeutic approach for diseases such as cancer. In order to understand the structure activity correlation of 2, 4, 6 pyridine based topoisomerase inhibitor, we have carried out a combined pharmacophore modelling, 3D-QSAR studies, molecular docking and virtual screening studies. A five point pharmacophore with hydrogen bond acceptor (A), hydrogen bond donor (D) and three aromatic rings (R 5, R 6, R 7) was used to derive a predictive atom based 3d-qsar model. The generated model had showed good correlation coefficient for training set and test set ($R^2=0.91$ and $Q^2=0.827$). It was also validated using enrichment factor (EF) and goodness of hit score (GH score) and was used for virtual screening of compounds from 'zinc drug like database'. Docking study of the hits retrieved from virtual screening revealed the binding affinity of these inhibitors at the active site of topoisomerase enzyme. *In silico* ADME predictions was also performed. These findings provide a set of guidelines for designing compounds with better topoisomerase inhibitory potential.

INTRODUCTION: DNA topoisomerases are ubiquitous enzymes playing a key role in solving topological problems associated with DNA molecule¹.

The extraordinary chain length of DNA and its double helical structure creates serious problems like twisting, knotting, tangling and super coiling during the process of replication, transcription and recombination.

DNA topoisomerases solves this problem by transiently breaking one or two strands through which the DNA strand can be passed in order to solve the topological problem and to relieve the torsion strain in DNA². There are two well-characterized classes of human topoisomerase. Topoisomerase I (Topo I) are monomeric which transiently break and relegate one strand of duplex DNA, while topoisomerase II (Topo II) are homodimeric and will break both strands of a duplex DNA. Type I and type II enzymes are fundamentally different in both mechanism and cellular function. A common feature of topoisomerases is their catalytic mechanism, which in all cases consists in a nucleophilic attack of a DNA phosphodiester bond by a catalytic tyrosyl residue from the topoisomerase³.

<p>QUICK RESPONSE CODE</p> 	<p>DOI: 10.13040/IJPSR.0975-8232.4(8).2939-54</p> <hr/> <p>Article can be accessed online on: www.ijpsr.com</p> <hr/> <p>DOI link: http://dx.doi.org/10.13040/IJPSR.0975-8232.4(8).2939-54</p>
---	--

These enzymes are highly expressed in rapidly proliferating tumor cells and, the medical importance of these enzymes is highlighted by the fact that they are the specific targets for many promising anticancer agents. Topoisomerase inhibitors are found to be the most efficient inducers of apoptosis⁴. Drugs that inhibit the topoisomerases include some of the most widely used anticancer drugs like irinotecan and topotecan which are known Topo I inhibitors and Topo II is the target for anticancer drugs like etoposide, teniposide, doxorubicin, idarubicin, epirubicin, and mitoxantrone.

Despite the wide use of Topo II targeted drugs as antitumour agents, several limitations hamper their benefits. Efforts for improving their clinical efficacy further by overcoming the drug resistance, myelosuppression and poor bioavailability problems associated with them, were continued to be challenging⁵.

Therefore, efforts have been made to develop novel topoisomerase inhibitors with a new scaffold distinct from existing drugs with improved bioactivity. The scaffold hopping strategy is a powerful approach for the discovery and modulation of medicinal ingredient by modifying the core structure of promising ligands⁶. Furthermore, this strategy not only gives the opportunity to modulate both selectivity and affinity of a given ligand but also allows the development and the exploitation of innovative chemistry in order to provide eventually new drugs. With this in mind, we selected 2, 4, 6 trisubstituted pyridine derivatives which are reported to possess topoisomerase I and II inhibitory activity along with strong cytotoxicity against several cancer cell lines like breast cancer adenocarcinoma, cervix tumor, Human prostate tumor, colorectal adenocarcinoma and myeloid leukemia.

Since these are the most common types of cancer, a good understanding of their chemical properties at the molecular level such as their lipophilic, steric, and electronic characteristics may provide important information on the anticancer properties of these analogues for further development. The discovery of new types of Topoisomerase inhibitors that can be synthesized easily, increased sensitivity in drug resistant tumors and decreased dose-limiting toxicities would be a significant

addition to the choices available in the treatment of cancer. Although a structure-based drug design approach is an attractive strategy, a ligand-based approach such as 3D-pharmacophore generation is useful for the identification of the pharmacophoric features which could help in designing new molecules⁷. Pharmacophore is an important and unifying concept in rational drug design that embodies the notion that molecules are active at a particular enzyme or receptor because they possess both a number of chemical features that favour the target interaction and geometry complementary to it⁸.

In our efforts towards finding potent topoisomerase inhibitor, we undertook a comprehensive molecular modelling study to identify the pertinent features that could serve as a starting point for design of ligands with increased affinity and target selectivity.

In this study, we have developed a quantitative pharmacophore model based on topoisomerase inhibitors collected from the literature. The best quantitative model was used as a 3D search query for screening the Zinc “clean drug-like” database to identify new topoisomerase inhibitors. Once identified, the candidate compounds were subsequently subjected to filtration using molecular docking to get drug like molecules.

MATERIAL AND METHODS:

Hardware and Software Specifications:

Molecular modeling studies were carried out on a personal computer running on windows⁷. Pharmacophore modeling and virtual screening experiments were performed using Schrodinger suite 2009 and modules like Phase, Ligprep, Quick Prop, Glide, and Virtual Screening Workflow were used in the study.

Data Base preparation:

Pharmacophore modelling correlates the spatial arrangement of various chemical features with their pharmacological effectiveness. It requires structural and activity data for a range of active and inactive molecules for generation of the hypothesis. For the pharmacophore modelling studies, a total of 72 molecules belonging to 2, 4, 6 tri substituted pyridine analogue having topoisomerase inhibitory activity were selected from the literature⁹⁻¹¹.

The reported anticancer activity (IC_{50}) against DU145, a human prostate tumor cell line was used and the IC_{50} value was converted into the corresponding PIC_{50} value.

IC_{50} is the dose in micromoles (μM) required to produce 50% inhibition. The structures of the 72 compounds used in this study, are given in **Table 1**.

TABLE 1: DATASET ANALYZED WITH EXPERIMENTAL AND PREDICTED ACTIVITIES

Sl. No.	Entry	R_2	R_4	R_6	IC_{50} (μM)	Observed Activity	Predicted Activity	Pharm set	QSAR set
1	Ligand-01				29.87	4.52	4.43	Inactive	Training
2	Ligand-02				26.68	4.57	4.69	Inactive	Training
3	Ligand-03				30.44	4.52	4.54	Inactive	Training
4	Ligand-04				20.09	4.7	4.74		Training
5	Ligand-05				14.75	4.83	4.73		Training
6	Ligand-06				17.23	4.76	4.65		Training
7	Ligand-07				33.44	4.48	4.51	Inactive	Test
8	Ligand-08				18.51	4.73	4.81		Training
9	Ligand-09				20.34	4.69	4.7		Training
10	Ligand-10				25.32	4.6	4.44		Test
11	Ligand-11				16.41	4.78	4.7		Training
12	Ligand-12				22.96	4.64	4.7		Test
13	Ligand-13				29.47	4.53	4.57	Inactive	Training
14	Ligand-14				20.52	4.69	4.7		Training
15	Ligand-15				18.49	4.73	4.65		Test

16	Ligand-16	27.31	4.56	4.58	Inactive	Training
17	Ligand-17	20.52	4.69	4.79		Test
18	Ligand-18	21.93	4.66	4.7		Training
19	Ligand-19	30.81	4.51	4.45	Inactive	Training
20	Ligand-20	27.67	4.56	4.65	Inactive	Test
21	Ligand-22	21.57	4.66	4.73		Training
22	Ligand-23	22.98	4.64	4.73		Training
23	Ligand-25	21.07	4.68	4.72		Training
24	Ligand-26	13.01	4.89	4.79		Training
25	Ligand-27	37.59	4.42	4.51	Inactive	Training
26	Ligand-28	21.84	4.66	4.74		Training
27	Ligand-29	19.27	4.72	4.76		Training
28	Ligand-30	16.82	4.77	5		Test
29	Ligand-31	18.10	4.74	4.82		Training
30	Ligand-32	9.18	5.04	4.77		Training
31	Ligand-33	12.98	4.89	4.88		Test

32	Ligand-34	18.86	4.72	4.64		Training
33	Ligand-35	18.50	4.73	4.63		Test
34	Ligand-36	24.76	4.6	4.58		Training
35	Ligand-37	17.92	4.75	4.91		Training
36	Ligand-38	21.23	4.67	4.7		Test
37	Ligand-39	19.30	4.71	4.8		Training
38	Ligand-40	10.42	4.98	4.92		Test
39	Ligand-41	19.53	4.71	4.49		Training
40	Ligand-42	10.94	4.96	4.96		Training
41	Ligand-43	21.57	4.66	4.63		Test
42	Ligand-44	1.48	5.83	5.48	Active	Test
43	Ligand-45	1.70	5.77	5.67	Active	Test
44	Ligand-46	1.97	5.7	5.74	Active	Training
45	Ligand-47	1.63	5.79	5.73	Active	Training
46	Ligand-51	2.75	5.56	5.26	Active	Test

47	Ligand-52	2.65	5.57	5.43	Active	Training
48	Ligand-53	3.33	5.47	5.65		Training
49	Ligand-54	2.02	5.69	5.63	Active	Training
50	Ligand-58	11.23	4.95	4.97		Training
51	Ligand-59	11.59	4.93	5.23		Training
52	Ligand-60	11.57	4.93	5.09		Training
53	Ligand-61	11.36	4.94	5.23		Test
54	Ligand-62	8.09	5.09	5.13		Training
55	Ligand-63	26.76	4.57	4.67	Inactive	Training
56	Ligand-64	2.51	5.6	5.32	Active	Training
57	Ligand-65	2.80	5.55	5.45	Active	Training
58	Ligand-66	4.19	5.37	5.38		Training
59	Ligand-67	3.89	5.41	5.25		Test
60	Ligand-68	5.30	5.27	5.15		Test

61	Ligand-72	5.36	5.27	5.21		Training
62	Ligand-73	5.74	5.24	5.2		Training
63	Ligand-74	6.22	5.2	5		Training
64	Ligand-75	5.75	5.24	5.27		Training
65	Ligand-76	35.20	4.45	4.44	Inactive	Training
66	Ligand-77	22.94	4.63	4.7		Training
67	Ligand-79	7.27	5.13	5.17		Training
68	Ligand-80	7.66	5.11	5.15		Test
69	Ligand-81	6.94	5.15	5.14		Test
70	Ligand-82	7.28	5.13	5.05		Training
71	Ligand-83	22.54	4.64	4.93		Test
72	Ligand-84	22.76	4.64	4.69		Training

Generation of the Common Pharmacophore Hypotheses (CPHs): Pharmacophore modelling provides a qualitative picture of the geometry of the active site by identifying the chemical features for binding of ligands and their spatial arrangements in 3D space¹². PHASE module of Schrodinger software¹³ was used to generate 3D Pharmacophore models and QSAR studies for the present series of compounds.

The structures of 72 molecules were sketched using maestro builder toolbar and all ligands were cleaned using the default Maestro settings. For each molecule, a set of conformers were generated through a mixed Monte-Carlo multiple minimum (MCMC)/Low mode (LMO) with maximum number of 1000 conformers per structure using a process minimization of 100 steps and each minimized conformer was filtered through a

relative energy difference 10 kcal/mol relative to the global energy minimum conformer with a maximum atom deviation of 2.00 Å. After the generation of conformers, only one conformer was displayed and carried for the further analysis. As active compounds are normally considered while developing common pharmacophore hypothesis, a “pharmaset” was defined by setting an active and inactive thresholds of $PIC_{50} > 5.5$ for actives and $PIC_{50} < 4.6$ for inactives.

PHASE provides a built-in set of six pharmacophore features such as hydrogen bond acceptor (A), hydrogen bond donor (D), hydrophobic group (H), negatively ionizable (N), positively ionizable (P) and aromatic ring (R). Common pharmacophores were identified using a tree-based partitioning technique that groups together similar pharmacophores according to their inter site distances, i.e., the distances between pairs of sites in the pharmacophore^{14, 15}. A five-point common pharmacophore hypothesis was identified from all the conformations of the active ligands having identical set of features with very similar spatial arrangement keeping minimum inter site distance 2.0Å in a final box size of 1.0Å with requirement that all actives should match.

Generated common pharmacophore hypotheses were examined by scoring alignment of actives against a reference ligand by using default settings. Scoring function such as score active, score inactive and rescore were applied for all five-featured common pharmacophore hypotheses. The scoring procedure provided a ranking of different hypotheses from which further investigation was carried out for appropriate hypothesis with rational choice.

Building the 3D-QSAR model: An atom-based 3D-QSAR model is more useful in explaining the structure activity relationship than pharmacophore based 3D-QSAR as the latter does not consider ligand features beyond the pharmacophore model¹⁶. In atom-based 3D-QSAR, a molecule is treated as a set of overlapping van der Waals spheres. Each feature is categorized according to a simple set of rules:

- (a) Hydrogens attached to polar atoms are classified as hydrogen-bond donors (D);

- (b) Carbons, halogens, and C–H hydrogens are classified as hydrophobic/non-polar (H);
- (c) Atoms with an explicit negative ionic charge are classified as negative ionic (N);
- (d) Atoms with an explicit positive ionic charge are classified as positive ionic (P); and;
- (e) N, O, and hydrogen-bond acceptors are classified as electron withdrawing (W) and all other types of atoms are classified as miscellaneous (X).

All the common pharmacophore hypotheses successfully generated and scored to generate atom-based 3D-QSAR models by correlating the observed and estimated activity for the set of 51 training molecules using PLS analysis. The PLS regression was carried out using PHASE with a maximum of PLS factor 5 and a grid spacing of 1.0Å. All models were validated by predicting activity of the set of 21 test molecules. The 3D-QSAR was evaluated by cross validated R^2 , Q^2 , SD, RMSE and Pearson- R . The predicted PIC_{50} at 5th PLS factor are tabulated in Table 2.

Evaluation of Pharmacophore model: The generated pharmacophore model should be statistically significant, predict activity of the molecules accurately, and it should also differentiate active and inactive compounds from a database. Therefore, the derived pharmacophore was further validated using the hit list (Ht), number of active percent of yields (%Y), percent ratio of actives in the hit list (%A), enrichment factor (EF), false negatives, false positives, and goodness of hit score (GH scoring method)¹⁷.

A decoy set including 1001 molecules with unknown activity and 15 active compounds is prepared for this step. Enrichment Factor (EF) and Goodness of Hit Score (GH) were calculated to evaluate the hypothesis ADRRR.1. EF and GH were calculated using below equations:

$$GH \text{ Score} = [(Ha/4HtA)(3A + Ht) + (1 - ((Ht - Ha)/(D - A)))]$$

$$EF = (Ha/Ht)/(A/D)$$

Where Ht is the number of hits retrieved, Ha is the number of active molecules in the hit list; A

represents the number of active molecules present in the database and D stands for the total number of molecules in the decoy set. The GH score ranges from 0, which indicates the null model, to 1, which indicates the ideal model.

Database search for new hits: The best-ranked five-point pharmacophore model, ADRRR.1, was used as a search query to retrieve compounds with novel and desired chemical features from Zinc “clean drug-like” database¹⁸.

Protein preparation: The protein structure of human Topo II- α co-crystallised with DNA and etoposide (PDB code 3QX3, resolution 2.16 Å) complex was obtained from the RCSB PDB^{and} was prepared using the Protein Preparation Wizard of the Schrödinger suite. H-atoms were added to the protein, including the protons necessary to define the correct ionization and tautomeric states of amino acid residues such as Asp, Ser, Glu, Arg, and His. The missing side chains of residues were corrected using prime interface incorporated in Maestro.

For each structure, minimization was carried out with the Impact refinement module, using the OPLS-2005 force field to alleviate steric clashes that may exist in the structures. The minimization was terminated when the energy converged or the Root Mean Square Deviation (RMSD) reached a maximum cut off of 0.30 Å¹⁹. Topo-II complex, 3QX3 contains Mg²⁺ ions, and a co-crystallised DNA segment, which was retained during the docking study²⁰.

After protein preparation, receptor grid was set up, which was generated by employing the Receptor Grid Generation panel. All amino acids within 20 Å of the 3QX3 were included in the grid file generation. Since this protein was associated with ligand, the ligand was selected to define the position and size of the active site.

Docking study: Docking studies were performed by means of Glide v5.6²¹. It performs grid-based ligand docking with energetics and searches for favourable interactions between one or more typically small ligand molecules and a typically larger receptor molecule, usually a protein²². Glide provides three different levels of docking precision: HTVS, high-throughput virtual screening; SP, standard precision; and XP, extra

precision. Docking calculations were first performed in HTVS mode and subsequently in SP and XP mode. All the molecules were built within Maestro using the Built module and an exhaustive conformational search was carried out for all molecules using OPLS-2005 force field, imposing a cut-off of allowed value of the total conformational energy compared to the lowest-energy state. A minimization cycle for conjugate gradient and steepest descent minimizations was used with default value 0.05 Å for the initial step size and 1.00 Å for the maximum step size. In convergence criteria for the minimization, both the energy change criteria and gradient criteria were used with default values 10⁻⁷ and 0.001 kcal/mol, respectively.

Virtual screening and drug-likeness prediction: For the exploration of novel scaffolds with Topoisomerase inhibitory activity, an *in silico* screening of 10,384,703 compounds from Zinc ‘clean drug-like’ database with derived pharmacophore model as a query was performed. The search criteria for compounds included in this database were: $x \log p \leq 5.0$, molecular weight in the range of 150–500, H-bond donor’s ≤ 5 , H-bond acceptor’s ≤ 10 .

Finally, compounds with the good estimated activity values were retrieved from databases and obtained molecules were chosen for subsequent molecular docking studies using virtual screening workflow by applying various filters in order to get more drugs like molecules.

RESULT AND DISCUSSION: The aim of this study was to elucidate the 3D structural features of 2,4,6 tri substituted pyridine derivatives crucial for binding, by generating 3D pharmacophore and to quantify the structural features of topoisomerase inhibitors essential for biological activity by generating atom-based 3D QSAR model.

For the pharmacophore modelling and QSAR studies, we have used Phase module of Schrodinger suite. This hypothesis generated by Phase will also convey the relative binding of the ligands inside the active site of the receptor.

Hence, we have used conformation suggested by the hypothesis for generating 3D-QSAR model to identify overall aspects of molecular structure that govern the activity.

Generation of the common pharmacophore hypotheses (CPHs): For the generation of pharmacophore model, compounds in the active “pharmaset” are normally considered. We included nine compounds having $PIC_{50} > 5.5$ as active and $PIC_{50} < 4.6$ as inactives and used four minimum sites and six maximum sites to have optimum combination of sites or features common to the most active compounds. Sixteen common pharmacophore models were generated with

different combination of variants in which top three ranking models were considered based on survival-inactive score for further QSAR generation. The top model was found to be associated with the five-point hypotheses was having hydrogen bond acceptor (A), hydrogen bond donor (D) and three aromatic rings (R 5,R 6,R 7) and was denoted as ADRRR1 (**Fig. 1a**). The special arrangement of features along with their distance aligned on most active compound **44** are depicted in **Fig. 1b**.

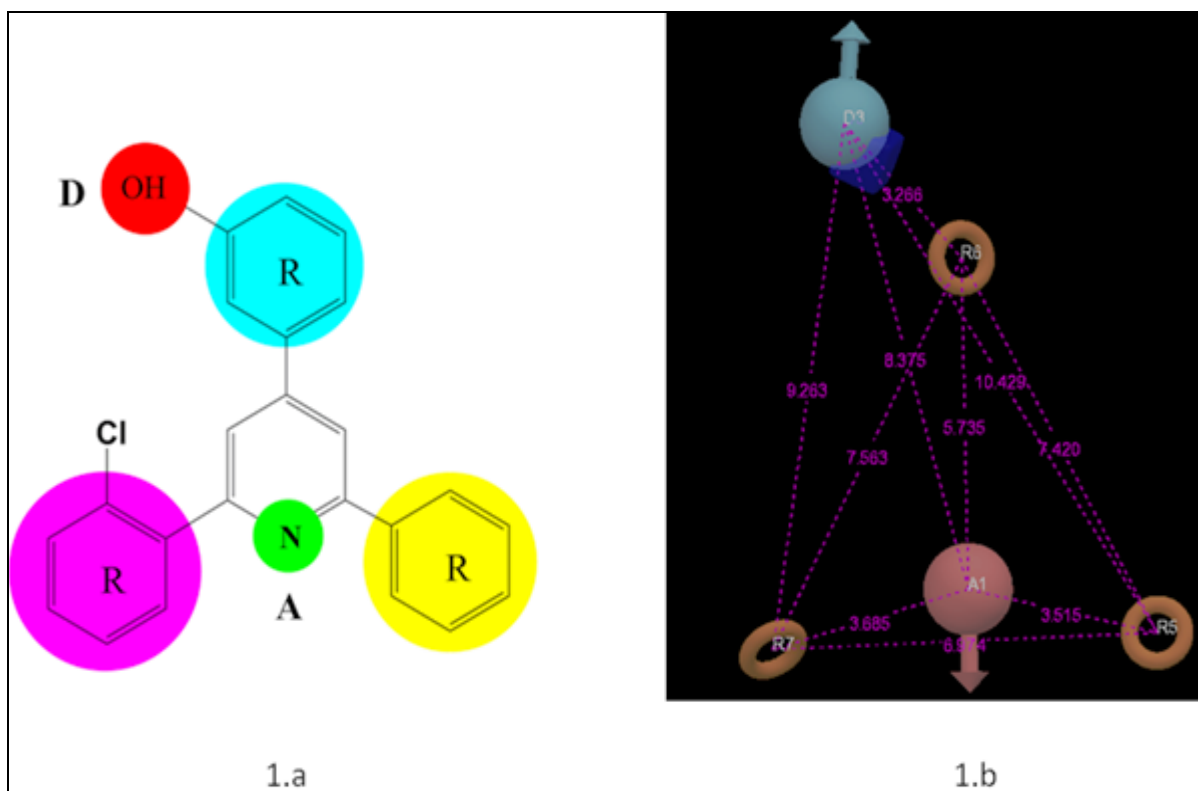


FIGURE 1A: GENERATED PHARMACOPHORE MODEL ADRRR1, FIGURE 1.B: PHARMACOPHORE HYPOTHESIS AND DISTANCE BETWEEN PHARMACOPHORIC SITES. ALL DISTANCES ARE IN Å UNIT.

The 72 molecules were divided into a training set (54 compounds) and a test set (18 compounds) for the purpose of atom-based 3D-QSAR. The training set molecules were selected in such a way that they contained information in terms of both structural features and biological activity ranges. The most active, several moderately active, and some inactive compounds were included in the training set in order to obtain critical information on pharmacophoric requirements²². In order to assess the predictive accuracy of the model, a set of 18 compounds was arbitrarily set aside as the test set. Training set compounds were aligned on the common pharmacophore hypotheses and analyzed by PLS with five factors. The predictivity of the generated 3D-QSAR model was analyzed by test set prediction.

Considering the flexibility of all the molecules, the predictive qualities of the QSAR model was satisfactory, based on R^2 , Q^2 , SD, and RMSE, as well as on the high value on the Pearson-R. The predicted and observed activities of the training and test set compounds are shown in **Figure 2**.

The training set correlation is characterized by PLS factors ($R^2 = 0.9101$, $SD=0.1168$, $F =91.1$, $P =2.175e-015$).

The test set correlation is characterized by PLS factors ($Q^2 =0.8276$, $RMSE=0.1633$, $Pearson-R =0.9159$).

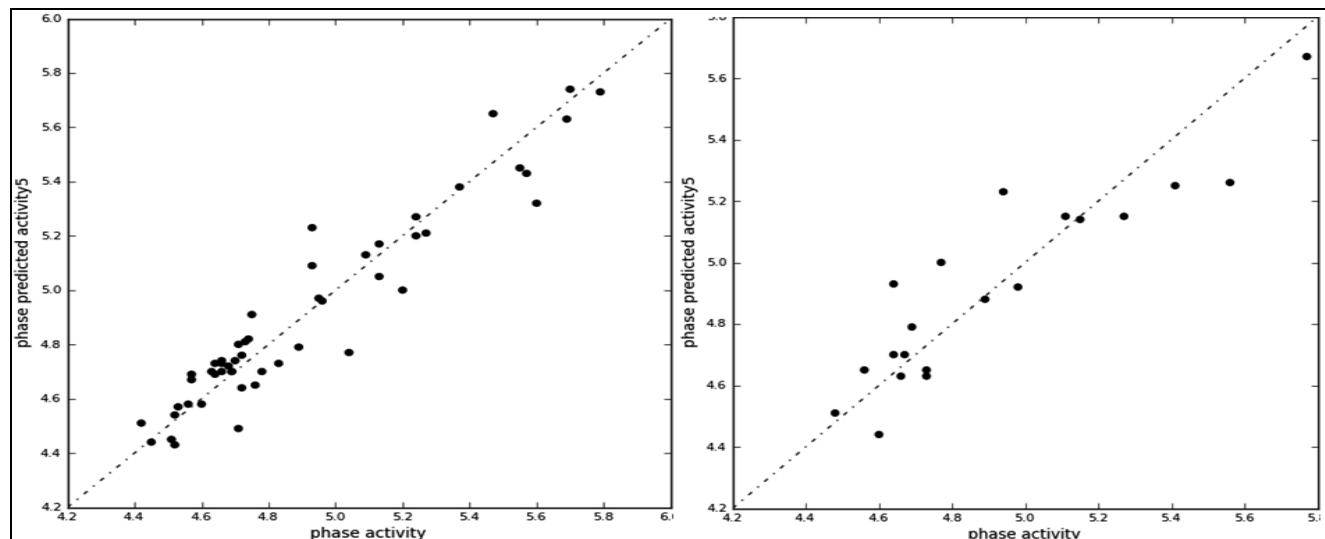


FIGURE 2: GRAPH OF OBSERVED VERSUS PREDICTED BIOLOGICAL ACTIVITY OF TRAINING SET AND TEST, RESPECTIVELY

The large value of F (91.1) indicates a statistically significant regression model, which is also supported by the small value of the variance ratio (P), an indication of a high degree of confidence. Further, small values of standard deviation (0.1168) of the regression and RMSE (RMSE = 0.1633) makes an obvious implication that the data used for model generation are best for the QSAR analysis. Validity of the model can be expressed by cross-validated correlation coefficient ($Q^2 = 0.8276$). The Q^2 value is more reliable and robust statistical parameter than R^2 because it is obtained by external validation method by dividing the dataset into training and test set.

The QSAR model displays 3D characteristics as cubes and the blue cubes indicate positive coefficients which are favourable while red cubes indicate negative coefficients which are

unfavourable regions for activity. This might give a clue to what functional group are desirable or undesirable at certain positions in a molecule. The blue cubes in 3D plots of the 3D pharmacophore regions refer to ligand regions in which the specific feature is important for better activity, whereas the red cubes demonstrates that particular structural feature or functional group, which is not essential for the activity or likely the reason for decreased binding potency.

The basic pyridine nucleus was found to be essential for the activity. The volume occlusion maps generated from 3D-QSAR studies highlight the structural features required for topoisomerases inhibition. when the QSAR model is applied to the most active compound 44 and least active compound 27 is shown in **figure 3(a-b)**.

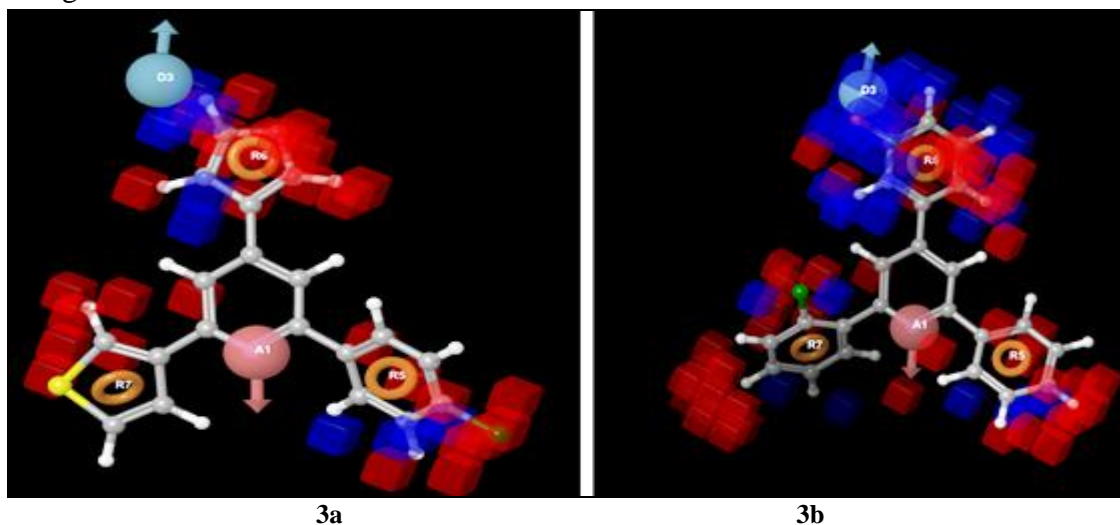


FIGURE 3: A. ATOM BASED 3D QSAR MODEL VISUALIZED IN THE CONTEXT OF MOST ACTIVE COMPOUND 44; B. LEAST ACTIVE COMPOUND 27 (BLUE CUBES INDICATE FAVOURABLE REGIONS WHILE RED CUBES INDICATE UNFAVOURABLE REGION FOR THE ACTIVITY)

Blue cubes were observed near the OH group of phenyl ring in ligand 44, suggesting that the presence such group at this position, capable of acting as hydrogen-bond donor, seemed to have a favourable effect on biological activity. Owing to the presence of this H-bond donor, compounds **11** and **39** are active. In the case of least active compound, 27 which was having a five member ring and also lacking the OH group.

It was reconfirmed by docking study, in the binding mode analysis of 44 with PDB 3QX3, H-bond contacts between Thiamine fragment (DT.D9) of DNA and the OH group of ligand 44 was observed. Most active compound 44 showed good binding affinity with the protein and the docking score was found to be -7.29 and for the least active compound it was -0.116.

Visual analysis demonstrates that the presence of the blue cubes at the phenyl ring, attached to 4th position of pyridine ring is pointing out the positive potential of hydrophobic group and is requisite for the activity at this particular place.

It can be suggested that addition of appropriate hydrophobic group at these positions, will append the topoisomerase inhibition, whereas the addition of hydrophobic groups on ring attached to 6th position of pyridine ring will contribute to decreased receptor binding.

The effect of H-bond donor, Hydrophobic, Electron-withdrawing substituents are given in **Figure 4**.

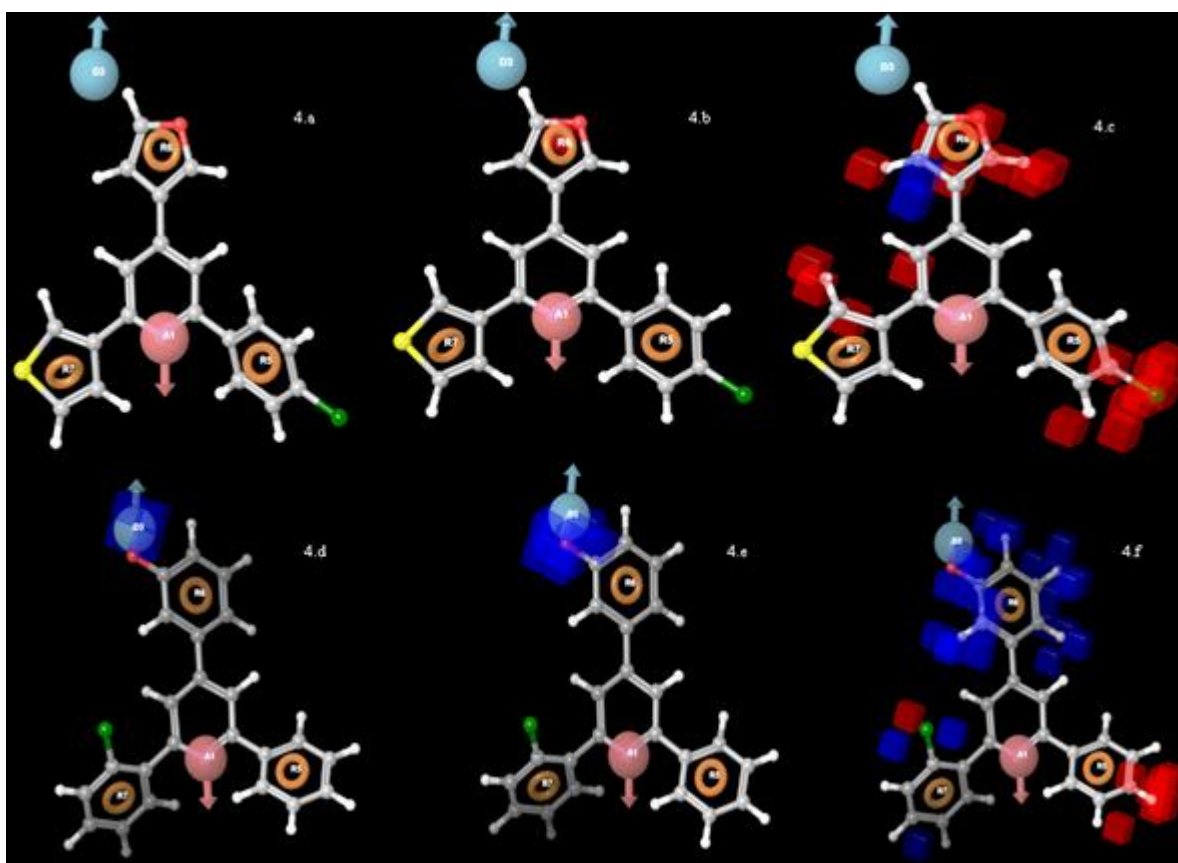


FIGURE 4A-F: EFFECT OF H-BOND DONOR, HYDROPHOBIC, ELECTRON-WITHDRAWING SUBSTITUENTS FOR COMPOUND 27; 4(A-C) AND FOR COMPOUND 44; 4(D-F). (BLUE CUBES: FAVOURABLE INFLUENCE ON ACTIVITY; RED CUBES: UNFAVOURABLE INFLUENCE ON ACTIVITY).

The predicted and actual activity was good for the developed model for both test and training set. The predictions of different activities have been classified according to the following residual scale (i.e. residual is computed as the difference between the experimental activity and the estimated activity): residuals less than 0.8 are considered as

good predictions; residuals between 0.8 and 1.6 are considered weak predictions and residuals higher than 1.6 are considered poor predictions.

In this study, residual scale (**figure 5**) was in the range of ± 0.3 which is an indication of a good model.

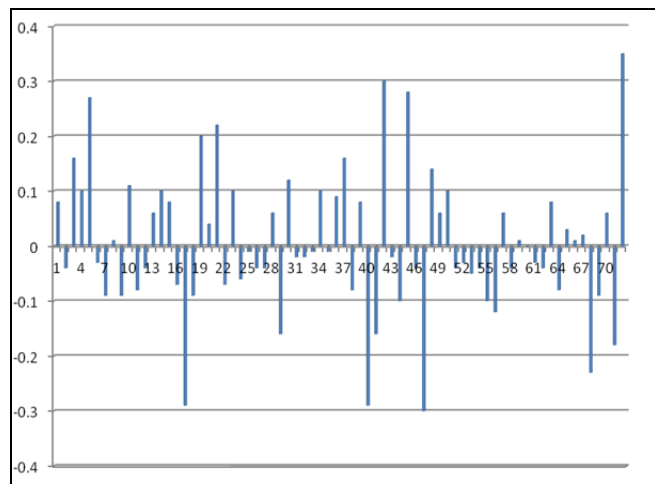


FIGURE 5: RESIDUAL SCALE

Assessment of Pharmacophore quality: The quality of pharmacophore was analyzed using a set of parameters such as hit list (Ht), number of active percent of yields (%Y), percent ratio of actives in the hit list (%A), enrichment factor (E), false negatives, false positives, and goodness of hit score (GH) (Table 4). The false positives and true negatives are 3 and 8 respectively. EF and GF are 48.38 and 0.78 respectively, When GH score is higher than 0.7, the model is very good indicated the quality of the model and high efficiency of the screening test.

TABLE 2: STATISTICAL PARAMETER FROM SCREENING DECOY SET

S. No.	Parameter	
1	Total number of molecules in database (D)	1016
2	Total number of actives in database (A)	15
3	Total number of hit molecules from the database (Ht)	21
4	Total number of actives molecules in the hit list (Ha)	15
5	% Yield of actives [(Ha/Ht) × 100] (%Y)	71.4
6	% Ratio of actives [(Ha/A) × 100] (%A)	100
7	Enrichment Factor (EF)	48.38
8	False negatives [A-Ha]	0
9	False Positives [Ht -Ha]	6
10	Goodness of Hit score (GH)	0.7809

Virtual screening: A pharmacophore-based virtual screening has been carried to find out potential topoisomerase inhibitors. Hypothesis ADRRR.1 was used to carry out a query of ZINC “drug-like” database of 10,384,703 molecules, which includes a wide variety of chemical scaffolds. The sequential virtual screening performed in this study is schematically represented in a flowchart in Figure 6, from which we can witness the number of hits reduced after each screening step.

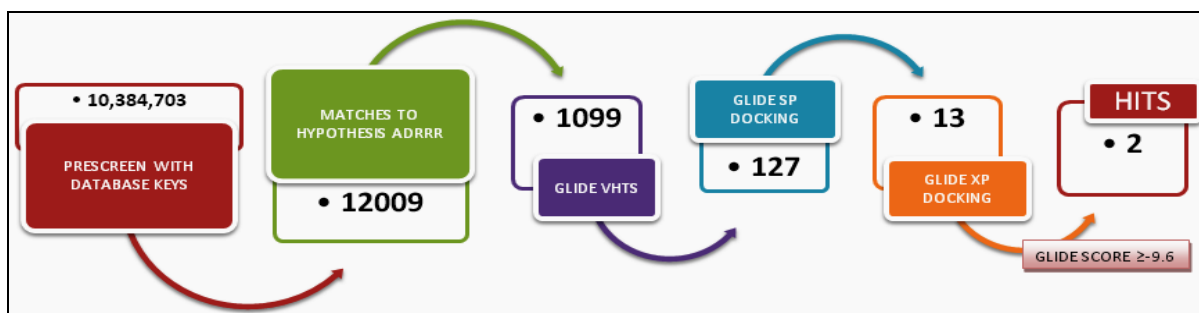
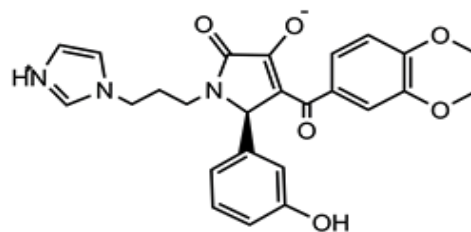


FIGURE 6: SCHEMATIZATION OF THE VS WORKFLOW

The initial filter using database query returned over 12009 hits. Next, various conformers of these hits were searched thoroughly for matches to pharmacophore model. While retrieving hits, matching of all five pharmacophoric features was made mandatory. A hit list of 1099 compounds matching the pharmacophore model was obtained. The virtual screening workflow (VSW) in Maestro was used to dock and to score the lead-like compounds. In the first step, Glide was run in high-throughput virtual screen mode. A total of 127 hits obtained after drug-likeness screening by the application of Lipinski's ‘rule of five’ and kept to go onto the next, Glide Single Precision (SP), stage.

The search retrieved 13 molecules were retained and docked using Glide Extra Precision (XP) mode. Among these, the molecules after visual inspection and estimated XP GlideScore ≥ -9.6 , were considered as potential topoisomerase inhibitors and are shown in Figure 7.



ZINC09009213

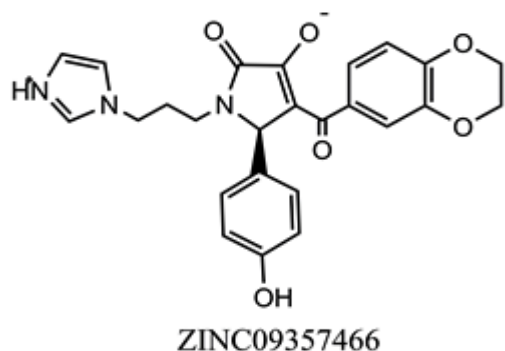


FIG. 7: POTENTIAL TOPOISOMERASE INHIBITORS

Docking study of hits: The ligand interaction diagram of most active hit compound (ZINC09009213) is shown in **Figure 8**. It is observed that both the lead molecules were able to occupy the same sites occupied by the co-crystallized ligand (etoposide) molecule, indicating

that this site was the most probable interaction site for these compounds. As presented in **Figure 9**, compound ZINC09009213 and ZINC09357466 are inserted between the base pairs of DNA and may effectively blocking religation of the cleaved phosphodiester bond and hence as etoposide, therefore, the docking results suggest that the DNA site in Topo II- α is the more probable binding site for this type of molecule. So a mechanism of action similar to that of etoposide can be proposed for these lead compounds.

TABLE 3: DOCKING SCORE OF SELECTED HITS:

Sl. No.	Entry ID	XP G Score	Docking score
1	ZINC09009213	-10.299378	-9.756578
2	ZINC09357466	-9.637271	-9.171671
5	Etoposide	-8.298543	-8.298543

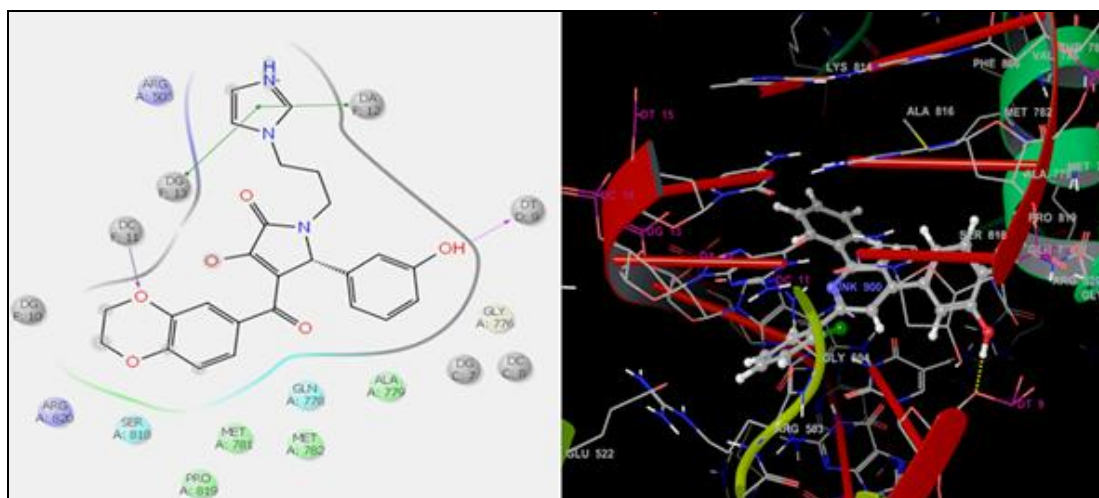


FIGURE 8: CRYSTAL STRUCTURE OF ZINC09009213 BOUND TO TOPOISOMERASE II (PDB: 3QX3)

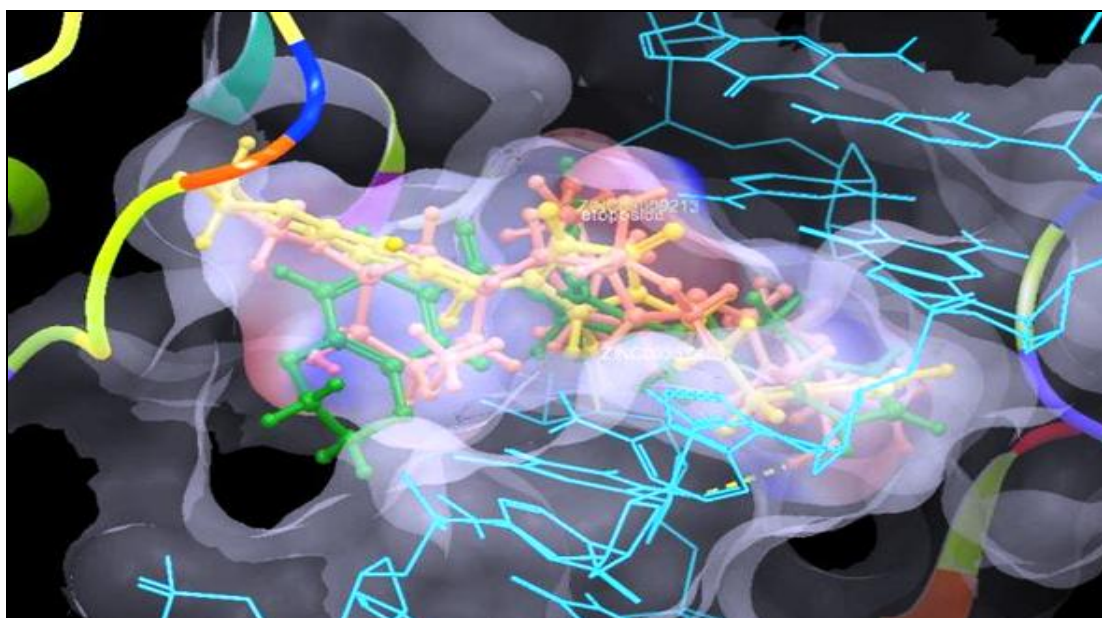


FIGURE 9: PICTORIAL REPRESENTATION OF THE GLIDE XP DOCKING OF COMPOUND ZINC09009213 (GREEN) ZINC09357466 (YELLOW) ALONG WITH ETOPOSIDE (ORANGE) INTO ACTIVE SITE OF TOPO-II

To validate the procedure, and adequate scoring function selection, the co-crystallised ligand etoposide was removed and redocked it into the receptor (PDB-3QX3). It was found that this structure, when superimposed on the crystal structure, has a root mean square deviation (RMSD) of only 0.065673Å. Docking score of all lead molecules and etoposide are shown in Table 3. It can be seen that two of the lead molecules were having docking score higher than that of etoposide.

Predicted ADME Properties: The ZINC database was evaluated for drug-likeness of the lead molecules by assessing their physicochemical properties and by applying Lipinski's rule of five. Their molecular weights were <500 Daltons with <5H-bond donors, <10H-bond acceptors and a log p of <5; these properties were well within the acceptable range of the Lipinski rule for the final lead molecules.

Drug-like behaviour of the potential leads was assessed by analysing pharmacokinetic parameters required for ADME using QikProp 3.2²⁴. QikProp is frequently used in *in-silico* screening studies for ADME analysis of potential leads²⁵. QikProp properties for the final hits were calculated.

The molecular weights of all the lead molecules were in the range of 424–461. QP log Po/w shows the partition coefficient, which is important for the estimation of absorption and distribution of drugs within the body. For the lead compounds, the partition coefficient (QPlogP o/w) and water solubility (QPlogS), critical for estimation of absorption and distribution of drugs within the body ranged between 3.264 to 4.527 and –5.258 to –6.286.

Cell permeability (QPPCaco), a key factor governing drug metabolism and its access to biological membranes, ranged from 29.7 to 1207.5. QPPMDCK value which are considered to be a good mimic for the blood brain barrier ranges from 77.853 to 310.456. Overall, the percentage human oral absorption for the compounds ranged from 86.47 to 100 %. The standard drug etoposide the predicted percentage human oral absorption was only 41.52% all the virtual lead molecules retrieved from virtual screening has showed betted oral absorption.

All lead molecules shown pharmacokinetic parameters within the acceptable range defined for human use (see **Table 4** footnote), thereby indicating their potential as drug-like molecules.

TABLE 4: ADME PROPERTIES OF SELECTED HITS

Zinc ID	QPlogPo/w ^a	QPPCaco ^b	QPlogS ^c	QPlogHERG ^d	QPPMDCK ^e	% Absorption ^f
09009213	3.268	180.725	-5.304	-6.668	77.853	86.47
09357466	3.264	182.223	-5.259	-6.618	78.551	86.51
Etoposide	-0.806	335.935	-2.375	-4.241	152.155	41.52

^aMolecular weight. ^aPredicted octanol/water partition co-efficient log p (acceptable range: –2.0 to 6.5). ^bPredicted Caco-2 cell permeability in nm/s (acceptable range , <25 is poor and >500 is great). ^cPredicted aqueous solubility; S in mol/L (acceptable range: –6.5 to 0.5).

CONCLUSION: In conclusion, A ligand-based pharmacophore model was generated for the series of 2, 4, 6 pyridine derivatives with topoisomerase inhibitory activity to reveal the structural features responsible for biological activity. A five-point pharmacophoric feature with three aromatic rings (R) and hydrogen bond acceptor (A), hydrogen bond donor (D) was developed and evaluated by 3D-QSAR model. It resulted in good statistical significance and predictive ability with $R^2 = 0.9101$ and $Q2 = 0.8276$. The developed pharmacophore was also validated using EF and GH score. Furthermore, visualization of the 3D-QSAR model in the context of the molecules under study provided details of the relationship between

structure and activity and thus provides explicit indications for the design of better analogues. We have also shown how straightforward virtual screening can be used to rapidly retrieve compounds with a desired activity from a large compound pool with limited experimental effort.

QikProp pharmacokinetic prediction provided physicochemical properties along with BBB permeability and percentage oral absorption. These parameters are helpful to find out bioavailability and toxicity prediction in human body. Compared with currently known active compounds, these newly identified inhibitors have significant potential for further development.

ACKNOWLEDGEMENT: The authors are thankful to University Grants Commission (UGC), New Delhi, for providing financial support through UGC Major Project.

REFERENCES:

1. Wang JC: Cellular roles of DNA topoisomerases. A molecular perspective. *Nature Reviews Molecular Cell Biology* 2002; 3:430-440.
2. Yves Pommier: *DNA Topoisomerases and Cancer*. Humana Press, First Edition 2012.
3. Yves Pommier: *DNA Topoisomerase I Inhibitors*. Chemistry, Biology and Interfacial Inhibition Chemical Reviews. 2009; 109: 2894–2902.
4. Sordet O, Khan QA, Kohn KW, Pommier Y: Apoptosis induced by Topoisomerase Inhibitors. *Current Medicinal Chemistry - Anti-Cancer Agents*. 2003; 4:271-290.
5. Naik PK, Dubey A, Soni K, Kumar R, Singh H: The binding modes and binding affinities of epipodophyllotoxin derivatives with human topoisomerase II α . *Journal of Molecular Graphics and Modelling*, 2010; 29:546–564.
6. Bohm HJ, Flohr A, Stahl M. Scaffold hopping. *Drug discovery Today: Technologies* 2004; 1:217–224.
7. Mustata GI, Brigo A, Briggs JM: HIV-1 integrase pharmacophore model derived from diverse classes of inhibitors. *Bioorganic Medicinal Chemistry Letters* 2004; 14:1447–1454.
8. Marriott DP, Dougall IG, Meghani P, Liu YJ, Flower DR: Lead generation using pharmacophore mapping and three dimensional database searching: application to muscarinic M3 receptor antagonists. *Journal of Medicinal Chemistry* 1999, 42:3210–3216.
9. Thapa P, Karki R, Yun M, Kadayat TM, Lee E, Kwon HB, Na Y, Cho WJ, Kim ND, Jeong BS, Kwon Y, Lee ES: Design, synthesis and antitumor evaluation of 2,4,6 triaryl pyridines containing chlorophenyl and phenolic moiety. *European Journal of Medicinal Chemistry* 2012, 52:123-136.
10. Thapa P, Karki R, Thapa U, Yurngdong J, Lee ES: 2-Thienyl-4-furyl-6-aryl pyridine derivatives: Synthesis, topoisomerase I and II inhibitory activity, cytotoxicity, and structure–activity relationship study. *Bioorganic Medicinal Chemistry* 2010; 18:377–386.
11. Thapa P, Karki R, Choi H, Cho JH, Lee ES. Synthesis of 2-(thienyl-2-yl or -3-yl)-4-furyl-6-aryl pyridine derivatives and evaluation of their topoisomerase I and II inhibitory activity, cytotoxicity, and structure–activity relationship. *Bioorganic Medicinal Chemistry*. 2010, 18:2245–2254.
12. Jain AK, Ravichandran VR, Vaidya A, Mourya V, Agrawal RK. QSAR analysis of some novel sulfonamides incorporating 1, 3, 5-triazine derivatives as carbonic anhydrase inhibitors. *Medicinal Chemistry Research* 2010, 19:1191-1202.
13. Phase, version 3.1, Schrödinger, LLC, New York 2009.
14. Dixon SL, Smondyrev AM, Rao SN: PHASE: a novel approach to pharmacophore modeling and 3D database searching. *Chemical Biology & Drug Design* 2006; 67:370–372.
15. Dixon SL, Smondyrev AM, Knoll EH, Rao SN, Shaw DE, Friesner RA: "PHASE: A New Engine for Pharmacophore Perception, 3D QSAR Model Development, and 3D Database Screening. Methodology and Preliminary Results, *The Journal of Computer-Aided Molecular Design* 2006; 20:647-671.
16. Teli MK and Rajanikant G K: Pharmacophore generation and atom-based 3D-QSAR of N-iso-propyl pyrrole-based derivatives as HMG-CoA reductase inhibitors. *Organic and Medicinal Chemistry Letters* 2012; 2:25.
17. Guner O.F., Henry D.R. Development, and Use in Drug Design. La Jolla: IUL Biotechnology Series, First edition 2000.
18. Irwin JJ, Shoichet BK; ZINC-a free database of commercially available compounds for virtual screening. *Journal of Chemical Information and Modeling* 2005; 45:177–182.
19. Wu CC, Li TK, Farh L, Lin LY, Lin TS, Yu YJ, Yen TJ, Chiang CW, Chan NL: Structural basis of type II topoisomerase inhibition by the anticancer drug etoposide. *Science* 2011, 22; 333:459-62.
20. Teli MK, Rajanikant GK, Identification of novel potential HIF-prolyl hydroxylase inhibitors by in silico screening. *Molecular Diversity* 2012; 16:193–202.
21. Esteves-Souza A, Claudio E. Santos R, Cistia CN, Silva DR, Carlos M R. Sant Anna: Solvent-Free Synthesis, DNA-Topoisomerase II Activity and Molecular Docking Study of New Asymmetrically *N,N'*-Substituted Ureas. *Molecules* 2012; 17:12882-12894.
22. Glide, version 5.5 (2009) Schrödinger, LLC, New York.
23. Golbraikh A, Shen M, Xiao Z, Xiao YD, Lee KH, Tropsha A. Rational selection of training and test sets for the development of validated QSAR models. *Journal of Computer Aided Molecular Design* 2003; 17:241-53.
24. QikProp, version 3.2, Schrödinger, LLC, New York, NY, 2009.
25. Bandgar B, Hote B, Gangwal R, Sangamwar A: Synthesis, biological evaluation, and pharmacokinetic profiling of benzophenone derivatives as tumor necrosis factor-alpha and interleukin-6 inhibitors. *Medicinal Chemistry Research* 2012; 21:1-5.

How to cite this article:

Dev S and Dhaneshwar SR: Identification of potent virtual leads as Topoisomerase-II inhibitors using Pharmacophore Modelling, Molecular Docking and ADME studies. *Int J Pharm Sci Res* 2013; 4(8); 2939-2954. doi: 10.13040/IJPSR.0975-8232.4(8).2939-54

All © 2013 are reserved by International Journal of Pharmaceutical Sciences and Research. This Journal licensed under a Creative Commons Attribution-NonCommercial-ShareAlike 3.0 Unported License.

This article can be downloaded to **ANDROID OS** based mobile. Scan QR Code using Code/Bar Scanner from your mobile. (Scanners are available on Google Playstore)